

Effective mechanical properties of micro/nano-scale porous materials considering surface effects

Joonho Jeong¹, Maenghyo Cho*² and Jinbok Choi³

¹*Interdisciplinary Program In Automotive Engineering, Seoul National University
Gwanangno 599, Sillim-9Dong, Kwanak-gu, Seoul 151-742, Korea*

²*School of Mechanical and Aerospace Engineering, Seoul National University*

³*Metal Forming Research Group, POSCO Global R&D Center, 180-1
Songdo-dong, Yeonsu-gu, Incheon, 406-840, Korea*

(Received November 11, 2010, Accepted February 18, 2011)

Abstract. Mechanical behavior in nano-sized structures differs from those in macro sized structures due to surface effect. As the ratio of surface to volume increases, surface effect is not negligible and causes size-dependent mechanical behavior. In order to identify this size effect, atomistic simulations are required; however, it has many limitations because too much computational resource and time are needed. To overcome the restrictions of the atomistic simulations and graft the well-established continuum theories, the continuum model considering surface effect, which is based on the bridging technique between atomistic and continuum simulations, is introduced. Because it reflects the size effect, it is possible to carry out a variety of analysis which is intractable in the atomistic simulations. As a part of the application examples, the homogenization method is applied to micro/nano thin films with porosity and the homogenized elastic coefficients of the nano scale thickness porous films are computed in this paper.

Keywords: multiscale analysis; surface effect; homogenization; porous materials.

1. Introduction

In recent years, advance in fabrication techniques enables to manufacture various micro/nano-sized structures. In accordance with small size, these structures can be useful to very high sensitive resonators or biochemical sensors in order to detect a molecule or a virus so that manufacturing research has been undertaken to this challenging field. However, micro/nano-sized structures exhibit very different material properties compared with macro- sized structures. Therefore, size-dependent material properties in the nano scales should be investigated to predict their behaviors and to study their important design issues.

A change of mechanical properties in nano-sized structures compared with macro-sized structures is due to surface effects. Atomistic bonding at an exterior surface is different from thoes in the interior bulk part as shown in Fig. 1. Atoms at the free surface of the film due to bonding loss are placed under an excessive energy state. Thus, it can be understood that surface effect is caused by

* Corresponding author, Professor, E-mail: mhcho@snu.ac.kr

the difference of atomic bonding energy between surface and bulk layers. Although this surface effects is negligible because it is a very small amount in the macro-sized materials, it becomes a crucial part in the nano scale structures.

It is demonstrated that mechanical properties show unique feature in various nano-sized structures such as nanowires, nanotubes or nanobeams (Cammarata and Sieradzki 1989). Miller and Shenoy (2000) showed that Young's modulus or bending stiffness in plates experience the dramatic change as the thickness of the plate becomes thinner. This phenomenon resulting from surface effects has been investigated in the previous work with both experiments and atomistic simulations (Wong *et al.* 1997, Poncharal *et al.* 1999).

As the computing power increases and the numerical techniques are improved, the molecular dynamics (MD) simulation has been used as the conventional method to analyze nano-sized structures; however, it is hard to design nano-sized structures in practical applications since it has still the difficulties in modeling and the limitations on the simulation size. Therefore, the continuum approach for nano-sized structures has become very attractive to many researchers. Gurtin and Murdoch (1975a, 1975b) proposed the continuum model taking into consideration of surface stress for homogeneous and isotropic materials. The elastic mechanical behaviors of nano-sized thin films are analyzed to adopt the surface elasticity model of Gurtin and Murdoch (Lim *et al.* 2004, Lu *et al.* 2006). Cho *et al.* (2009) and Choi *et al.* (2010) implemented the finite element formulation for nano-sized thin films based on Kirchhoff classical plate theory and predicted the thermo-mechanical properties accurately. Furthermore, various analysis methods based on continuum theory has been attempted to estimate more accurate dynamic response of nano resonators (Lim *et al.* 2009, Chen and Lee 2010). The developed continuum model considering surface effects is applicable to MEMS/NEMS structures from nano scale to micro scale. When connecting with the well-established continuum theories, the performance of nano-sized thin films can be predicted and it is expected that the design optimization can be efficiently performed.

In this paper, the homogenization method in linear elasticity problem is used to analyze the nano-sized thin films with porosity. The homogenization enables us to lead the equivalent material properties in composite materials; therefore, it is easier in the modeling task and it can save computational time. In general, the representation of effective material property for composite materials is based on the volume average technique over the representative volume element (RVE). Among various approaches of the homogenization, the two-scale method that is formulated by applying the asymptotic expansion method is adopted (Guedes and Kikuchi 1990, Hollister and Kikuchi 1992, Michel *et al.* 1999). Firstly, the modified Mindlin plate theory considering surface effects is introduced. Secondly, the homogenized elastic stiffness coefficients considering surface effects are predicted for the first time by the multiscale continuum model.

1. Continuum model considering surface effects

1.1 Mindlin plate theory considering surface effects

In Mindlin plate theory, the displacement fields are defined as follows

$$u_\alpha = u_\alpha^0 + z\psi_\alpha, \quad u_3 = u_3^0 \quad (1)$$

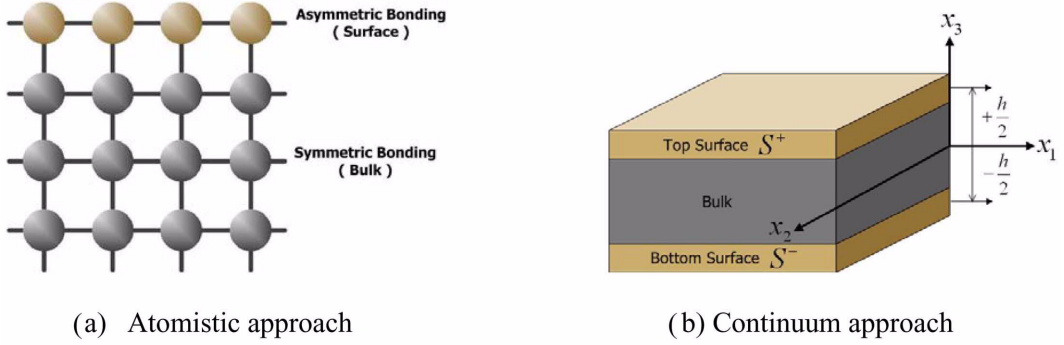


Fig. 1 Schematics of surface effect in atomistic and continuum approach

Top and bottom surface layers due to atomic bonding loss can be distinct from bulk layer as shown in Fig. 1. Therefore, it can be assumed that there are top and bottom surface layers (S^+ , S^-) at $x_3 = \pm h/2$ in order to model surface effects. From the displacement continuity conditions at the interface between bulk and surface layers, additional displacement fields at surface layers can be represented as

$$u_{\alpha}^{S^+} = u_{\alpha}|_{x_3 = +h/2} = (u_{\alpha}^0 + z\psi_{\alpha})|_{x_3 = +h/2} = u_{\alpha}^0 + \frac{h}{2}\psi_{\alpha}, \quad u_3^{S^+} = u_3^0 \quad (2a)$$

$$u_{\alpha}^{S^-} = u_{\alpha}|_{x_3 = -h/2} = (u_{\alpha}^0 - z\psi_{\alpha})|_{x_3 = -h/2} = u_{\alpha}^0 - \frac{h}{2}\psi_{\alpha}, \quad u_3^{S^-} = u_3^0 \quad (2b)$$

The equilibrium equation in thin films considering surface effects can be derived by the virtual work principle. For a static problem, the total virtual work takes the following form.

$$\delta\Pi = \delta U + \delta V \quad (3)$$

where δU and δV denote the variation of the internal strain energy and the external virtual work respectively.

The internal virtual work consists of bulk and surface layers parts and it can be expressed as Eq. (4) under the Mindlin plate assumption.

$$\begin{aligned} \delta U &= \delta U_{\text{bulk}} + \delta U_{\text{surface}} \\ &= \int_{\Omega} N_{\alpha\beta} \delta u_{\alpha,\beta}^0 + M_{\alpha\beta} \delta \psi_{\alpha,\beta} + Q_{\alpha} \delta \gamma_{\alpha} dA \\ &+ \int_{\Omega} (\sigma_{\alpha\beta}^{S^+} + \sigma_{\alpha\beta}^{S^-}) \delta u_{\alpha,\beta}^0 + \frac{h}{2} (\sigma_{\alpha\beta}^{S^+} - \sigma_{\alpha\beta}^{S^-}) \delta \psi_{\alpha,\beta} + (\sigma_{\alpha 3}^{S^+} + \sigma_{\alpha 3}^{S^-}) \delta \gamma_{\alpha} dA \\ &= \int_{\Omega} N_{\alpha\beta}^* \delta u_{\alpha,\beta}^0 + M_{\alpha\beta}^* \delta \psi_{\alpha,\beta} + Q_{\alpha}^* \delta \gamma_{\alpha} dA \end{aligned} \quad (4)$$

where $N_{\alpha\beta}$, $M_{\alpha\beta}$ and Q_{α} are stretching, moment and transverse shear resultants, respectively and if the coefficients are rearranged, the resultants can be newly defined as

$$N_{\alpha\beta}^* = N_{\alpha\beta} + \sigma_{\alpha\beta}^{S+} + \sigma_{\alpha\beta}^{S-}, \quad M_{\alpha\beta}^* = M_{\alpha\beta} + \frac{h}{2}(\sigma_{\alpha\beta}^{S+} - \sigma_{\alpha\beta}^{S-}), \quad Q_{\alpha}^* = Q_{\alpha} + \sigma_{\alpha 3}^{S+} + \sigma_{\alpha 3}^{S-} \quad (5)$$

On one hand, the external mechanical force distributions are considered in the external work done so that the external virtual work is given by

$$\delta V = \int_{\Omega} (p_{\alpha} \delta u_{\alpha}^0 + p_3 \delta w) dA \quad (6)$$

From Eqs. (4) and (6), the final variational equations can be obtained and if the divergence theorem and the integration by parts are applied, the following expression is obtained.

$$\begin{aligned} \delta \Pi &= \int_{\Omega} -(N_{\alpha\beta}^* + p_{\alpha}) \delta u_{\alpha}^0 - (M_{\alpha\beta}^* - Q_{\alpha}^*) \delta \psi_{\alpha} - (Q_{\alpha, \alpha}^* + p_3) \delta w dA \\ &= \int_{\Gamma} N_{\alpha\beta}^* \nu_{\beta} + M_{\alpha\beta}^* \nu_{\beta} \delta \psi_{\alpha} + Q_{\alpha}^* \nu_{\alpha} \delta w dS \end{aligned} \quad (7)$$

where ν_{α} is the normal vector component along of the boundary of the thin film.

The Euler-Lagrange equations are obtained from the first term in Eq. (7) as follows

$$\delta u_{\alpha}^0: N_{\alpha\beta, \beta}^* + p_{\alpha} = 0, \quad \delta \psi_{\alpha}: M_{\alpha\beta, \beta}^* - Q_{\alpha}^* = 0, \quad \delta w: Q_{\alpha, \alpha}^* + p_3 = 0 \quad (8)$$

and the boundary line integral term in Eq. (7) provides the boundary conditions along the edge of the thin film.

1.2 The constitutive equations for the continuum model considering surface effects

The constitutive equation for homogeneous and isotropic materials, which corresponds to a bulk layer, is given by

$$\sigma_{ij} = \lambda \varepsilon_{kk} \delta_{ij} + 2\mu \varepsilon_{ij} \quad (9)$$

where λ and μ are Lamé's constants.

The constitutive equation at a surface layers is derived by Gurtin and Murdoch (1975a, 1975b, 1978). If the top and bottom surface layers are the same material, it is expressed as

$$\sigma_{\alpha\beta}^{S\pm} = \tau_0 \delta_{\alpha\beta} + (\mu_0 - \tau_0)(u_{\alpha, \beta}^{S\pm} + u_{\beta, \alpha}^{S\pm}) + (\lambda_0 + \tau_0) u_{\gamma, \gamma}^{S\pm} \delta_{\alpha\beta} + \tau_0 u_{\alpha, \beta}^{S\pm} \quad (10)$$

where τ_0 is the surface residual tension which induces to reach self-equilibrium positions of atoms under the unstrained state and λ_0 , μ_0 denote the surface Lamé's constants. The constitutive equation as shown in Eq. (10) is valid only to the isotropic materials. Thus, Eq. (10) cannot be applied to nano-sized films which have single crystal structures because these structures have anisotropy. In general, the shear modulus is not related to Young's modulus and Poisson's ratio in case of body centered cubic (BCC) or face centered cubic (FCC) structures. For this reason, Eq. (10) should be modified to satisfy cubic materials as following equations.

$$\sigma_{\alpha\beta}^{S\pm} = \tau_0 \delta_{\alpha\beta} + ((\mu_0)_{\alpha\beta} - \tau_0)(u_{\alpha, \beta}^{S\pm} + u_{\beta, \alpha}^{S\pm}) + (\lambda_0 + \tau_0) u_{\gamma, \gamma}^{S\pm} \delta_{\alpha\beta} + \tau_0 u_{\alpha, \beta}^{S\pm} \quad (11)$$

where

$$(\mu_0)_{\alpha\beta} = (\mu_0^e - \mu_0^s) \delta_{\alpha\beta} + \mu_0^s \quad (12)$$

1.3 Finite element formulation

From Eqs. (5) and (8), the constitutive equations related to stretching, moment and transverse shear resultants can be constructed. Thus, using the variational equation as show in Eq. (7), the finite element formulation for the nano thin films can be derived as follows

$$\begin{aligned} & \int_{\Omega} \delta d_m^T \mathbf{B}_m^T \mathbf{A}_m \mathbf{B}_m d_m - \delta d_b^T \mathbf{B}_b^T \mathbf{D}_b \mathbf{B}_b d_b + d_s^T \mathbf{B}_s^T \mathbf{A}_s \mathbf{B}_s d_s dA \\ & = - \int_{\Omega} 2 \tau_0 \delta d_m \mathbf{B}_m dA + \int_{\Omega} \delta d_m^T \mathbf{N}^T p_\alpha + \delta d_b^T \mathbf{N}^T p_3 dA \end{aligned} \quad (13)$$

where subscript m , b and s denotes membrane, bending and shear parts respectively and \mathbf{A}_m , \mathbf{D}_b and \mathbf{A}_s are the stretching stiffness, bending stiffness and transverse shear stiffness respectively. As shown in Eq. (11), four surface parameters in the constitutive equation must be determined to implement analysis of nano-sized thin films considering surface effects. Determination of surface parameters accompanies atomistic calculation and the detail procedure will be mentioned in the numerical examples section.

2. Homogenization

The homogenization method is useful to determine the equivalent elastic constants in porous materials and it promotes to do more effective modeling process. By the virtual work principle, the problem of deformation of an elastic body can be written by

$$\int_{\mathbf{V}} C_{ijkl} \partial u_{k,x_i} \partial \delta u_{l,x_j} d\mathbf{V}_x = \int_{\mathbf{V}} b_i \delta u_i d\mathbf{V}_x + \int_{\Gamma} t_i \delta u_i d\Gamma_i + \int_S p_i \delta u_i dS - \int_{\Omega} 2 \tau_0 \delta u_i d\Omega \quad (14)$$

When the material has the repetitive RVE patterns, two distinct coordinates which consist of macroscopic variable X and the microscopic variable y are introduced as shown Figs. 2 and 3. If the non-dimensional small parameter is defined as

$$\varepsilon = x/y \quad (15)$$

the displacement field can be expressed by applying the asymptotic expansion with respect to ε as follows

$$u^\varepsilon(x) = u^0(x, y) + \varepsilon u^1(x, y) + \varepsilon^2 u^2(x, y) + \dots \quad (16)$$

The assumption that the size of the RVE is very small compared with the size of an elastic body $\varepsilon \ll 1$ satisfies y -periodicity, and if Eq. (16) is substituted into Eq. (14) and terms with the same power of ε are rearranged by considering up to the first order displacement, the following equation set can be obtained.

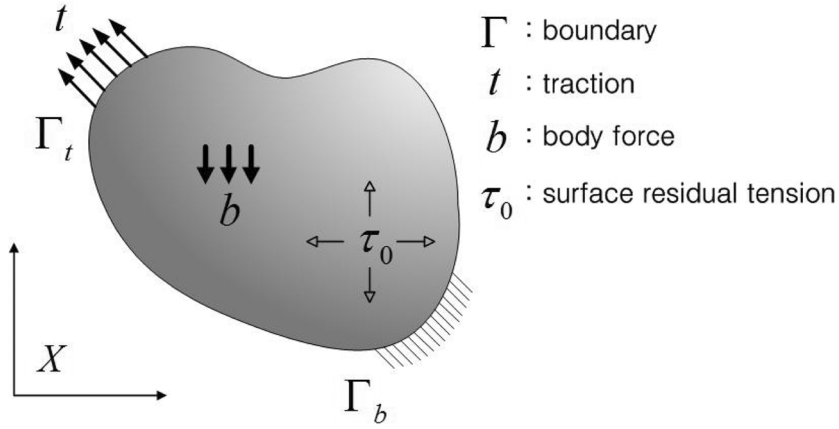


Fig. 2 Elastic body

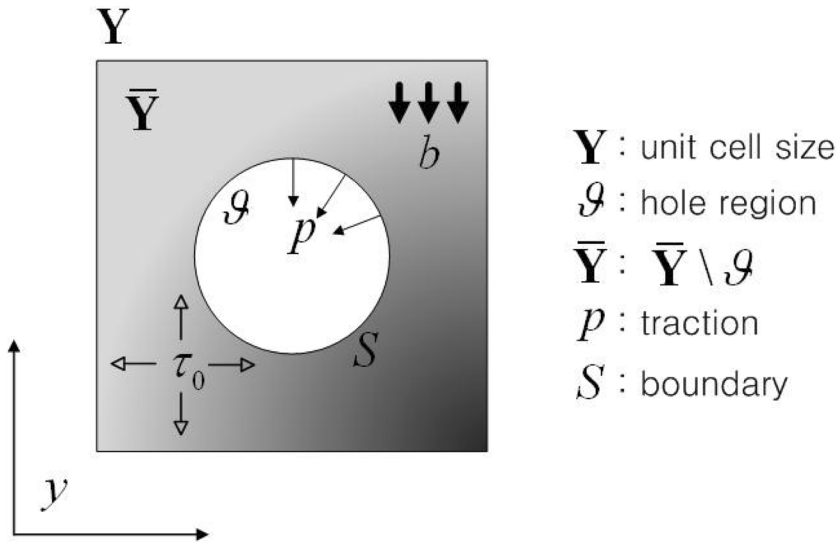


Fig. 3 Representative volume elements of porous materials

$$O(1/\varepsilon^2): \int_{\mathbf{v}} \frac{1}{Y} \left[\int_{\bar{Y}} C_{ijkl} \frac{\partial u_k^0}{\partial y_l} \frac{\partial \delta u_i}{\partial y_j} d\mathbf{v}_y \right] d\mathbf{v}_x = 0 \quad (17a)$$

$$\begin{aligned}
 O(1/\varepsilon): \int_{\mathbf{v}} \frac{1}{Y} \left[\int_{\bar{Y}} C_{ijkl} \left\{ \left(\frac{\partial u_k^0}{\partial x_l} + \frac{\partial u_k}{\partial y_l} \right) \frac{\partial \delta u_i}{\partial y_j} + \frac{\partial u_k^0}{\partial y_l} \frac{\partial \delta u_i}{\partial x_j} \right\} d\mathbf{Y} \right] d\mathbf{v}_x \\
 = \int_{\mathbf{v}} \frac{1}{Y} \left[\int_S p_i \delta u_i dS \right] d\mathbf{v}_x \quad (17b)
 \end{aligned}$$

$$\begin{aligned}
 O(1): & \int_{\mathbf{V}} \frac{1}{\mathbf{Y}} \left[\int_{\bar{\mathbf{Y}}} C_{ijkl} \left\{ \left(\frac{\partial u_k^0}{\partial x_l} + \frac{\partial u_k^1}{\partial y_l} \right) \frac{\partial \delta u_i}{\partial x_j} + \left(\frac{\partial u_k^1}{\partial x_l} + \frac{\partial u_k^2}{\partial y_l} \right) \frac{\partial \delta u_i}{\partial y_j} \right\} d\mathbf{Y} \right] d\mathbf{V}_x \\
 & = \int_{\mathbf{V}} \frac{1}{\mathbf{Y}} \int_{\bar{\mathbf{Y}}} b_i d\mathbf{Y} d\mathbf{V}_x - \int_{\mathbf{V}} \frac{1}{\mathbf{Y}} \int_{\bar{\mathbf{Y}}} 2 \tau_0 d\mathbf{Y} d\mathbf{V}_x
 \end{aligned} \quad (17c)$$

The displacement u_k^0 in Eq. (17a) represents only macroscopic mechanical behavior and the displacement u_k^1 that can be obtained by the differential equation in Eq. (17b) is related to fluctuation due to inhomogeneity. If there is no applied traction on S inside the RVE, only the particular solution remains and the displacement u_k^1 can be expressed as

$$u_k^1 = -\chi_i^{kl} \frac{\partial u_k^0}{\partial x_l} \quad (18)$$

where the third order tensor χ_i^{kl} which expresses warping deformation under a unit initial strain can be calculated by

$$\int_{\bar{\mathbf{Y}}} C_{ijkl} \frac{\partial \chi_k^{qr}}{\partial y_l} \frac{\partial \delta u_i}{\partial y_j} d\mathbf{Y} = \int_{\bar{\mathbf{Y}}} C_{ipqr} \frac{\partial \delta u_i}{\partial y_p} d\mathbf{Y} \quad (19)$$

If the body force is ignored, the variational equation in Eq. (14) can be rewritten by substituting Eq. (18) into Eq. (17c) as follows

$$\int_{\Omega} C_{ijkl}^H \frac{\partial u_k^0(x)}{\partial x_l} \frac{\partial \delta u_i(x)}{\partial x_j} d\mathbf{V}_x = \int_{\Gamma_i} t_i(x) \frac{\partial \delta u_i(x)}{\partial x_j} d\Gamma - \int_{\Omega} 2 \tau_0(x) \frac{\partial \delta u_i(x)}{\partial x_j} d\mathbf{V}_x \quad (20)$$

where the homogenized elastic tensor is given by

$$C_{ijkl}^H(x) = \frac{1}{\mathbf{Y}} \int_{\bar{\mathbf{Y}}} \left(C_{ijkl} - C_{ijpq} \frac{\partial \chi_p^{kl}}{\partial x_q} \right) d\mathbf{Y} \quad (21)$$

3. Numerical Examples

The configuration of RVE which has a circular hole is shown in Fig. 4. As the size of a hole changes (Table 1), the homogenized elastic coefficients considering surface effects are compared with the results without including surface effects.

3.1 Determination of surface parameters

The surface parameters, which give rise to size dependence of mechanical properties, can be determined by experiments or MD simulations. In this paper, the parameters are identified by MD simulations with open source code (LAMMPS). The material in this study is the single crystal copper which has the face centered cubic (FCC) crystal structure. In the first stage, the atoms are

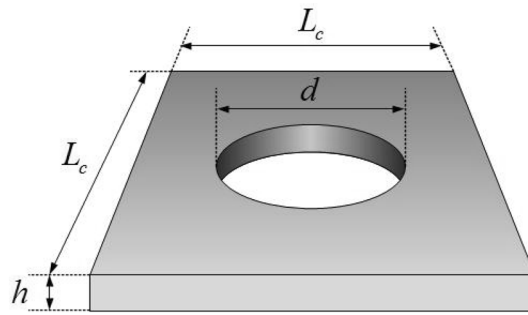


Fig. 4 Configuration of the RVE

Table 1 Dimension of a hole inside the RVE and volume fraction

Diameter of a hole	Volume fraction
0.2 L_c	0.969
0.3 L_c	0.929
0.4 L_c	0.874
0.5 L_c	0.804
0.6 L_c	0.717
0.7 L_c	0.615
0.8 L_c	0.497

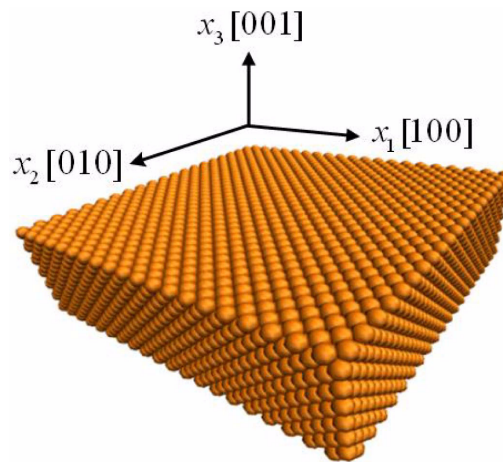


Fig. 5 Unit cell configuration of single crystal copper for MD simulations

arranged with the (100) crystallographic orientation and the unit cell configuration is shown in Fig. 5. In order to carry out atomistic simulations for a thin film, periodic boundary conditions are applied to in-plane directions; the $x_1[100]$ and $x_2[010]$ directions, and the free boundary conditions is applied to the out-of-plane direction; the $x_3[001]$ direction. And then, enough relaxation time with NPT ensemble (the number of atoms (N), pressure (P) and temperature (T) of the system are fixed)

is allowed to come to atomistic equilibrium positions during 100 ps. The constitutive matrix for FCC Cu with (100) lattice orientation is represented by three independent elastic coefficients. Contrast to isotropic materials, shear modulus is an independent engineering constant. Therefore, not only the tensile simulation but also the tilting simulations should be performed and the embedded-atom method (EAM) potential is applied to each simulation with NVT ensemble (the number of atoms (N), volume (V) and temperature (T) of the system are fixed). Furthermore, since the constitutive equation proposed by Gurtin and Murdoch in Eq. (10) can be applied to only isotropic materials, an additional surface parameter μ_0^s is introduced to satisfy shear modulus as shown in Eqs. (11) and (12). Four surface parameters can be extracted from the difference between the results of MD simulations and the bulk values as the following equations.

$$\begin{Bmatrix} N_{11}^* \\ N_{22}^* \\ N_{12}^* \end{Bmatrix} = \begin{Bmatrix} 2\tau_0 \\ 2\tau_0 \\ 0 \end{Bmatrix} + \begin{bmatrix} A_{11} & A_{12} & A_{16} \\ A_{12} & A_{22} & A_{26} \\ A_{16} & A_{26} & A_{66} \end{bmatrix} \begin{Bmatrix} u_{1,1}^0 \\ u_{2,2}^0 \\ u_{1,2}^0 + u_{2,1}^0 \end{Bmatrix} \quad (22)$$

where

$$A_{11} = A_{22} = \frac{Eh}{(1-\nu^2)} + 4\mu_0^e + 2\lambda_0, \quad A_{12} = \frac{E\nu h}{(1-\nu^2)} + 2\lambda_0 + 2\tau_0 \quad (23)$$

$$A_{66} = Gh + 2\mu_0^s - \tau_0, \quad A_{16} = A_{26} = 0 \quad (24)$$

In case of FCC structures, lattice orientation makes different mechanical properties. A thin film with (100) lattice orientation has the same directional properties in both [100] and [010] loading directions; however, different directional properties are exhibited at other loading direction and both [100] and [110] loading directions are considered in this paper.

From the constitutive equation obtained by MD simulations, the extensional stiffness matrix $[A]$ is constructed and deformation due to relaxation results from a surface residual tension τ_0 . At first, a surface residual tension τ_0 value can be determined by the Eq. (25) and its values agrees well with the previous research approximately (Streitz *et al.* 1994, Dingreville and Qu 2007).

$$\begin{Bmatrix} -2\tau_0 \\ -2\tau_0 \\ 0 \end{Bmatrix} = \begin{bmatrix} A_{11} & A_{12} & A_{16} \\ A_{12} & A_{22} & A_{26} \\ A_{16} & A_{26} & A_{66} \end{bmatrix} \begin{Bmatrix} \varepsilon_{11} \\ \varepsilon_{22} \\ 2\varepsilon_{12} \end{Bmatrix} \quad (25)$$

Therefore, three unknowns remain and they can be extracted by using three equations given in Eq. (22). The extracted surface parameters from MD simulations are summarized in Tables. 2 and 3. The surface parameter fitting values vary according to the thickness of the film as shown in Table 2. However, the variation of the parameter values is not significant in the characterization of the mechanical property because the mechanical properties of thin film are not significantly changed for the tabulated values of the identified surface parameters given in Table 2. In the present study, we select the values of surface parameters at the thickness 14.46 Å (the number of lattice = 4). After surface parameters are identified, it is possible to analyze nano-sized thin films considering surface

Table 2 Surface parameter values for (100) / <100>

(unit : N/m)

Number of lattice	τ_0	λ_0	μ_0^e	μ_0^s
4	1.613	23.321	-6.474	11.621
8	1.520	24.910	-7.302	12.242
12	1.490	25.231	-7.404	14.414
16	1.455	22.843	-7.124	15.648
Dingreville and Qu (2007)	1.398			

Table 3 Surface parameter values for (100) / <110>

(unit : N/m)

Number of lattice	τ_0	λ_0	μ_0^e	μ_0^s
4	1.508	2.468	9.710	-6.378
8	1.431	2.478	8.738	-6.864
12	1.421	2.668	8.340	-8.243
16	1.362	2.843	10.616	-8.965
Dingreville and Qu (2007)	1.398			

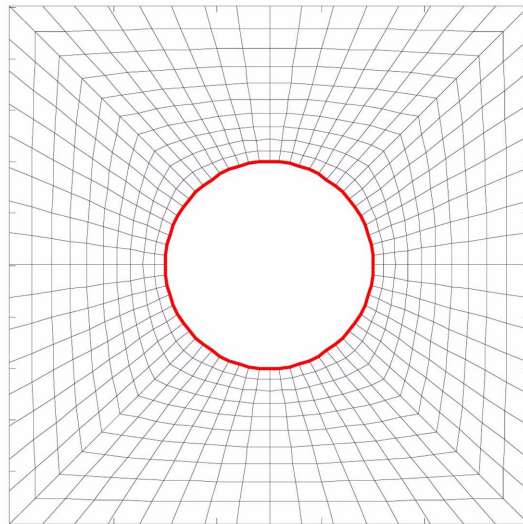


Fig. 6 Mesh configuration and line elements

effects by using FE model. As the thickness decreases, the change of mechanical properties due to surface effects can be predicted (Cho *et al.* 2009, Choi *et al.* 2010).

3.2 Surface effects generated from a hole boundary

To predict mechanical properties of nano-sized thin films with porosity more accurately, surface effects generated from a hole boundary should be considered. In this case, additional internal virtual

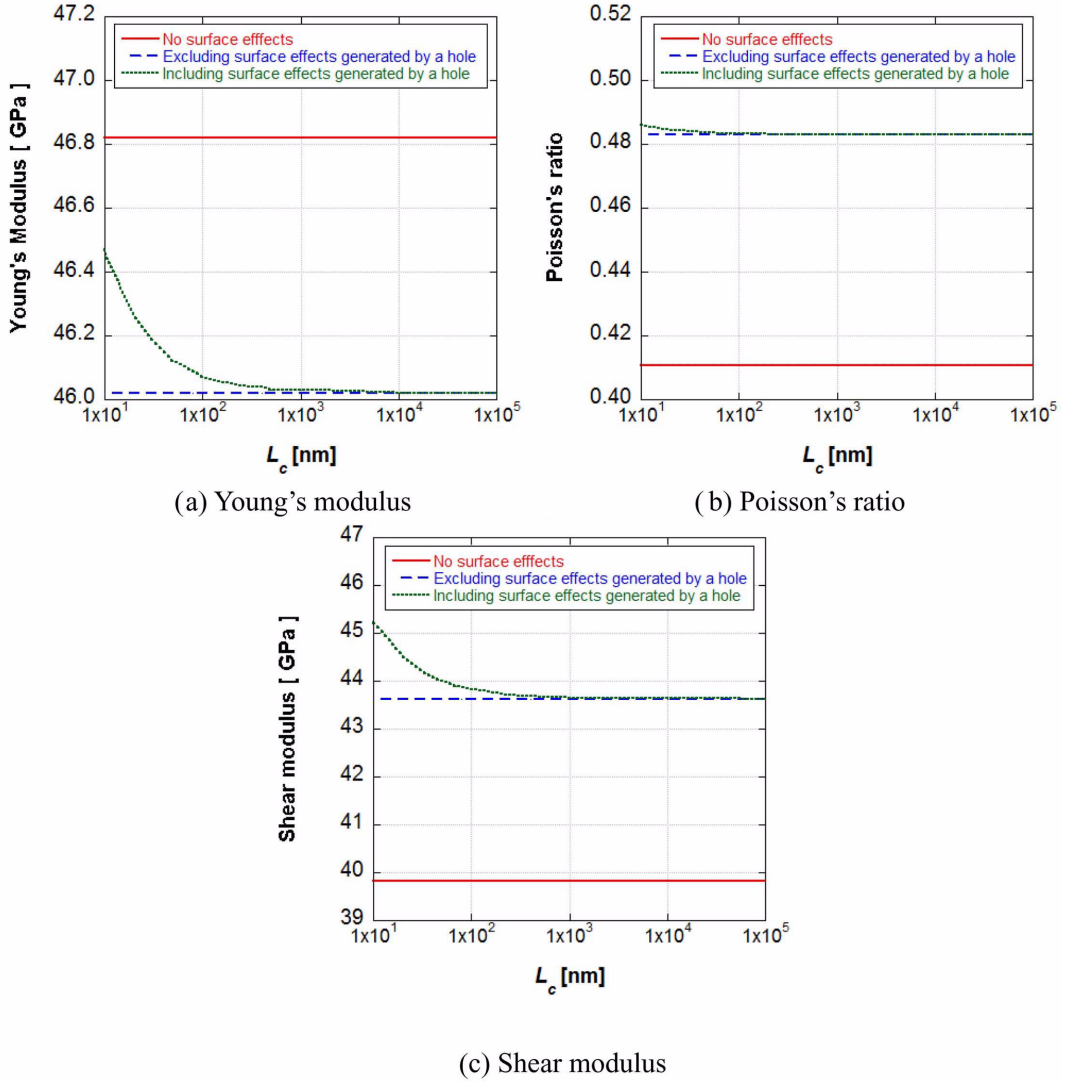


Fig. 7 Comparison of mechanical properties of nano thickness film with a hole inside the RVE about $\langle 100 \rangle$ direction with (100) surface orientation via the size of the RVE

work that comes from an increment in surface area should be put into the total internal virtual work.

$$\delta U = \delta U_{\text{bulk}} + \delta U_{\text{surface}} = \delta U_{\text{bulk}} + \delta(U_{\text{surface}}^{\text{top \& bottom}} + U_{\text{surface}}^{\text{hole boundary}}) \quad (26)$$

where

$$\delta U_{\text{surface}}^{\text{hole boundary}} = \int \sigma_{ss}^S \delta u_{s,s}^S h ds \quad (27)$$

In order to consider surface effects due to a hole in finite element formulation, line elements can

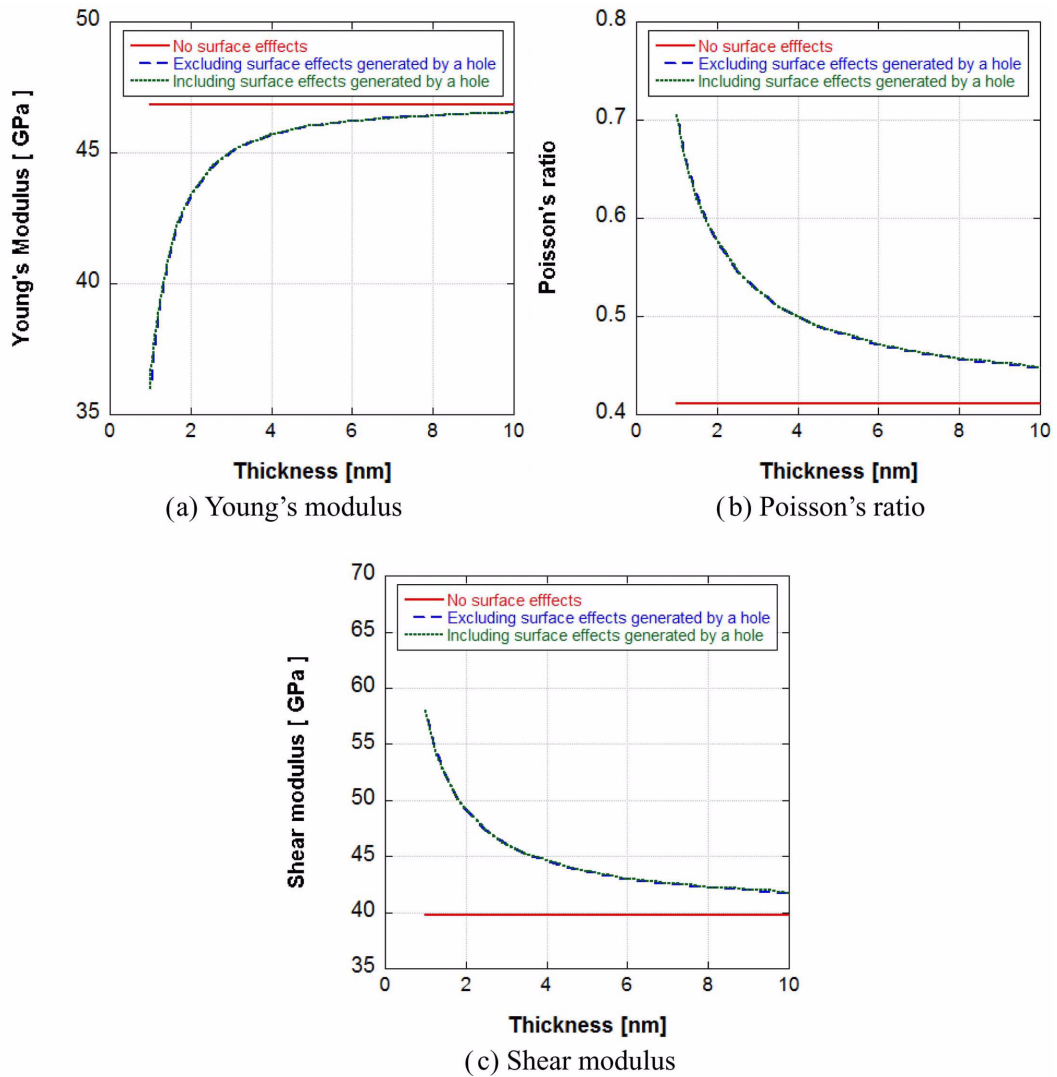
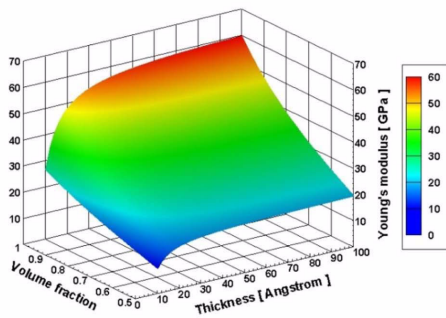
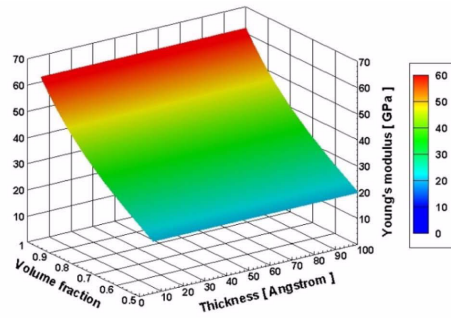


Fig. 8 Comparison of mechanical properties of nano thickness film with a hole inside the RVE about $\langle 100 \rangle$ direction with (100) surface orientation via the thickness of the RVE

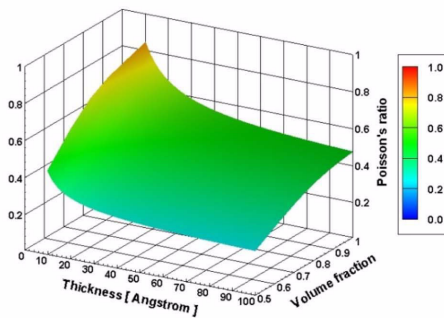
be added into boundary region around a hole (Gao *et al.* 2006). Surface effects has influence the change of mechanical behavior as the ratio of surface area to volume increases; thus, if the size of RVE increases or the thickness decreases, the surface effects due to a hole boundary becomes negligible. The line elements represented by red line along the boundary around a hole are added inside the RVE as shown in Fig. 6. The mechanical properties are examined in Fig. 7 when the thickness $h = 5\text{ nm}$ is fixed as the side length L_c of the RVE changes. In this case, the surface effects due to a hole almost vanishes when L_c is close to $1\ \mu\text{m}$. Fig. 8 shows that the surface effects due to a hole is not significant practically when L_c is $1\ \mu\text{m}$.



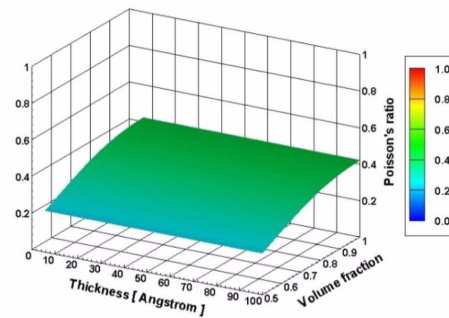
(a) Young's modulus with surface effects



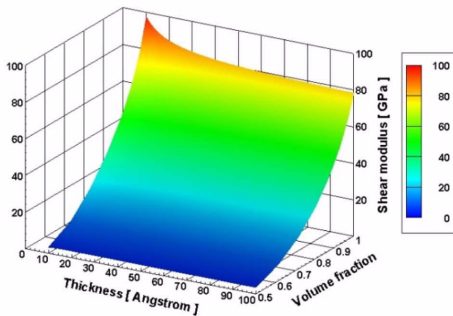
(b) Young's modulus without surface effects



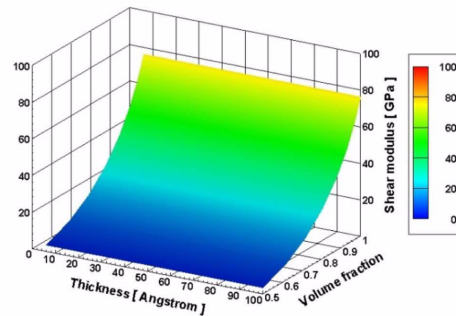
(c) Poisson's ratio with surface effects



(d) Poisson's ratio without surface effects



(e) Shear modulus with surface effects



(f) Shear modulus without surface effects

Fig. 9 Homogenized elastic coefficients with (100) surface orientation and $\langle 100 \rangle$ direction

3.3 Homogenized elastic constants considering surface effects

If the size of the RVE is small, the surface effects due to a hole cannot be neglected since the proportion of the area around a hole over total surface area becomes large. However, if the size of the RVE reaches hundreds of nanometer, that is, the hole size is within submicro scale, the amount of the surface effects due to a hole is negligibly small. Under the assumption that the RVE is in

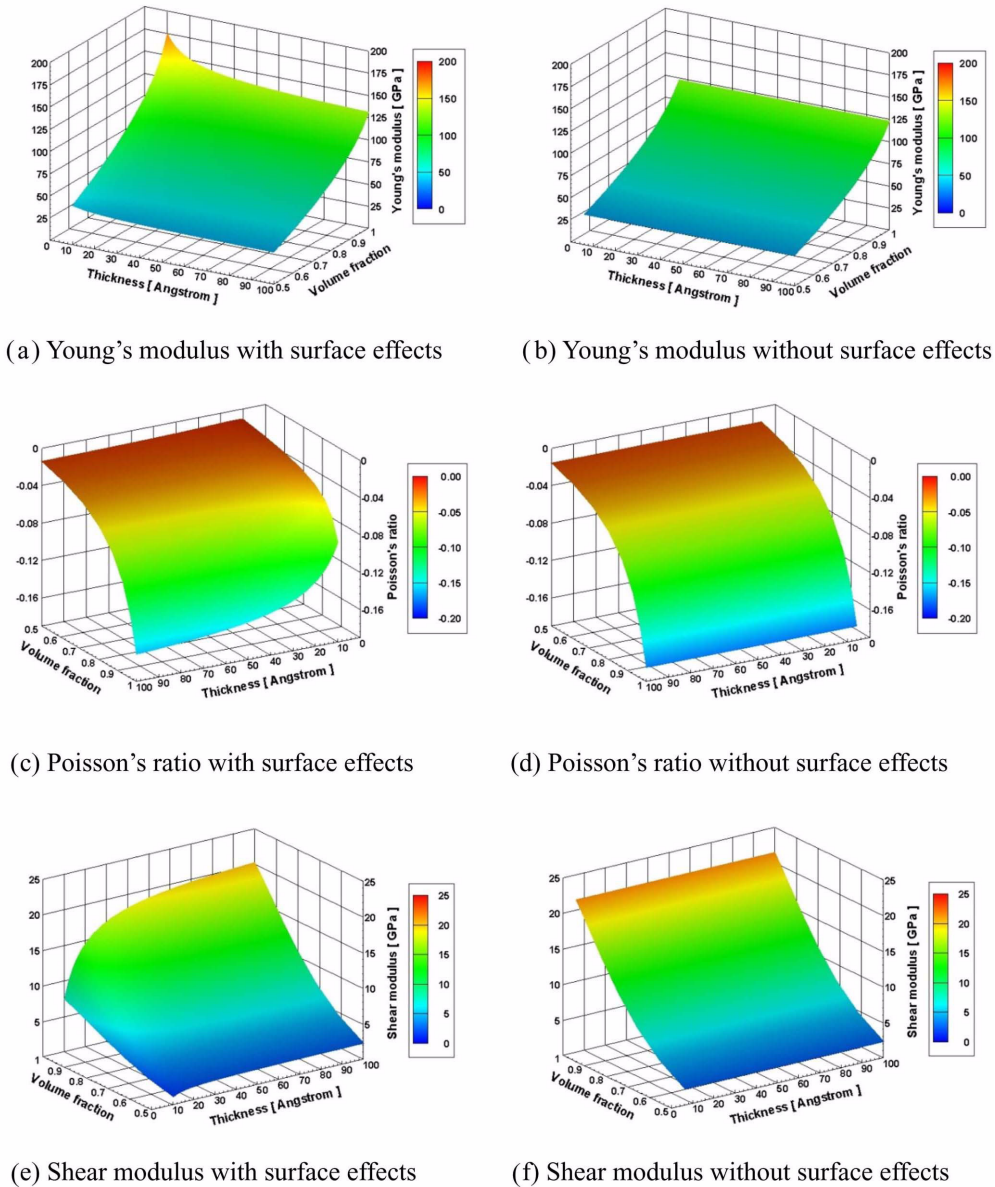


Fig. 10 Homogenized elastic coefficients with (100) surface orientation and $\langle 110 \rangle$ direction

submicro scale or micro scale size to disregard the surface effects generated from a hole boundary, the homogenized elastic constants considering surface effects are examined for the variation of two parameters, that is, the volume fraction and the thickness. Fig. 9 corresponds to [100] loading direction with (100) lattice orientation and Fig. 10 shows the results of [110] loading direction with (100) lattice orientation. Young's modulus, Poisson's ratio and shear modulus for porous materials are computed and Figs. 9 and 10(b), 10(d) and 10(f) are relevant to consideration of the surface effects and Figs. 9 and 10(a), 10(c) and 10(e) are the mechanical properties of the bulk part.

4. Conclusions

In order to investigate the size-dependent characteristics in the nano scale thin films, the established continuum model was combined with a surface elasticity. The first order Mindlin plate model was modified by correlating the surface parameters with those of MD simulations, hence elaborate MD simulations are required to identify the surface parameters. Although more accurate analysis depends on MD simulations, the overall tendency and numerical values agrees well with the previously reported results (Miller and Shenoy 2000, Cho *et al.* 2009, Choi *et al.* 2010). Because that continuum model considering surface effects is suitable to various application problems, it can be applicable much more efficiently than atomistic approaches such as molecular statics/dynamics methods. In this paper, the prediction of mechanical behavior for porous materials is carried out by the homogenization method. Topology optimization of the porosity shape is now under progress.

References

- Cammarata, R.C. and Sieradzki, K. (1989), "Effects of surface stress on the elastic moduli of thin films and superlattices", *Phys. Review Lett.*, **62**(17), 2005-2008.
- Cammarata, R.C. (1994), "Surface and interface stress effects in thin films", *Prog. Surf. Sci.*, **46**(1), 1-38.
- Chen, J. and Lee, J.D. (2010), "Atomistic analysis of nano/micro biosensors", *Interact. Multiscale Mech.*, **3**(2), 111-121.
- Cho, M., Choi, J. and Kim, W. (2009), "Continuum-based bridging model of nanoscale thin film considering surface effects", *JPN. J. Appl. Phys.*, **48**, 020219.
- Choi, J., Cho, M. and Kim, W. (2010), "Multiscale analysis of nano-scale thin film considering surface effects : thermomechanical properties", *J. Mech. Mater. Struct.*, **5**(1), 161-183.
- Dingreville, R., Qu, J. and Cherkaous, M. (2005), "Surface free energy and its effect on the elastic behavior of nano-sized particles, wires and films", *J. Mech. Phys. Solids*, **53**, 1827-1854.
- Dingreville, R. and Qu, J. (2007), "A semi-analytical method to compute surface elastic properties", *Acta Materialia*, **55**, 141-147.
- Gao, W., Yu, S. and Huang, G. (2006), "Finite element characterization of the size-dependent mechanical behavior in nanosystems", *Nanotechnology*, **17**, 1118-1122.
- Guedes, J.M. and Kikuchi, N. (1990), "Preprocessing and postprocessing for materials based on the homogenization method with adaptive finite element methods", *Comput. Method. Appl. M.*, **83**, 143-198.
- Gumbsch, P. and Daw, M.S. (1991), "Interface stresses and their effects on the elastic moduli of metallic multilayers", *Phys. Rev. B.*, **44**(8), 3934-3938.
- Gurtin, M.E. and Murdoch, A.I. (1975), "A continuum theory of elastic material surfaces", *Arch. Ration. Mech. An.*, **57**, 291-323.
- Gurtin, M.E. and Murdoch, A.I. (1975), "Addenda to our paper : a continuum theory of elastic material surface", *Arch. Ration. Mech. An.*, **57**, 291-323.
- Gurtin, M.E. and Murdoch, A.I. (1978), "Surface stress in solids", *Int. J. Solids Struct.*, **14**, 431-440.
- Hassani, B. (1996), "A direct method to derive the boundary conditions of the homogenization equation for symmetric cells", *Commun. Numer. Meth. Eng.*, **12**, 185-196.
- Hassani, B. and Hinton, E. (1998), "A review of homogenization and topology optimization II – analytical and numerical solution of homogenization equations", *Comput. Struct.*, **69**, 719-738.
- Hollister, S.J. and Kikuchi, N. (1992), "A comparison of homogenization and standard mechanics analyses for periodic porous composites", *Comput. Mech.*, **10**, 73-95.
- Michel, J.C., Moulinec, H. and Suquet, P. (1999), "Effective properties of composite materials with periodic microstructure : a computational approach", *Comput. Method. Appl. M.*, **172**, 109-143.
- Miller, R.E. and Shenoy, V.B. (2000), "Size dependent elastic properties of nanosized structural elements", *Nanotechnology*, **11**, 139-147.

- Lim, C.W. and He, L.H. (2004), "Size-dependent nonlinear response of thin elastic films with nano-scale thickness", *Int. J. Mech. Sci.*, **46**, 1715-1726.
- Lu, P., He, L.H., Lee, H.P. and Lu, C. (2006), "Thin plate theory including surface effects", *Int. J. Solids Struct.*, **43**(16), 4631-4647.
- Lim, C.W., Li, C. and Yu, J.L. (2009), "The effects of stiffness strengthening nonlocal stress and axial tension on free vibration of cantilever nanobeams", *Interact. Multiscale Mech.*, **2**(3), 223-233.
- Poncharal P., Wang Z., Ugarte, D. and deHeer, W.A. (1999), "Electrostatic deflections and electromechanical resonance of carbon nanotubes", *Science*, **283**, 1513-1516.
- Shenoy, V.B. (2005), "Atomistic calculations of elastic properties of metallic fcc crystal surfaces", *Phys. Rev. B.*, **71**(9), 094104.
- Simmons, G. and Huang, G.L. (1971), *Single crystal elastic constants and calculated aggregate properties : a handbook*, MIT Press, Cambridge, MA.
- Streitz, F.H., Cammarata, R.C. and Sieradzki, K. (1994), "Surface-stress effects on elastic properties. I. Thin metal films", *Phys. Rev. B.*, **49**(15), 10699-10706.
- Streitz, F.H., Sieradzki, K. and Cammarata, R.C. (1990), "Elastic properties of thin fcc films", *Phys. Rev. B.*, **41**(17), 12285-2287.
- Wong, E., Sheehan, P.E. and Liever, C.M. (1997), "Nanobeam mechanics : elasticity, strength, and toughness of nanorods and nanotubes", *Science*, **277**, 1971-1975.